The AAPS Journal, Vol. 18, No. 4, July 2016 (© 2016)
DOI: 10.1208/s12248-016-9919-9

Research Article

Dual Outcomes of Rosiglitazone Treatment on Fatty Liver

Mingming Gao,[1] Yongjie Ma,[1] Mohammad Alsaggar,[1] and Dexi Liu[1,2]

Received 10 February 2016; accepted 15 April 2016; published online 28 April 2016

Abstract. In previous studies, it has been reported that rosiglitazone has opposing effects on nonalcoholic fatty liver disease. The purpose of the current study is to test the hypothesis that such opposing effects are related to different levels of peroxisome proliferator-activated receptor gamma (PPAR-γ) in the liver. Using a gene transfer approach and mice fed a high-fat diet (HFD) as an animal model, we demonstrate that mice with low levels of PPAR-γ expression in the liver are resistant to HFD-induced development of fatty liver when treated with rosiglitazone. Conversely, rosiglitazone treatment actually exacerbates liver steatosis in obese mice that have a higher level of PPAR-γ. Mechanistic studies show that an elevated hepatic PPAR-γ level is associated with an increased expression of genes responsible for lipid metabolism in the liver, particularly *Cd36*, *Fabp4*, and *Mgat1*. The concurrent transfer of these three genes into the mouse liver fully recapitulates the phenotypic change induced by the overexpression of PPAR-γ. These results provide evidence in support of the importance of PPAR-γ in the liver when rosiglitazone is considered for the treatment of fatty liver disease. Clinically, our results suggest the necessity of verifying PPAR-γ levels in the liver when rosiglitazone is considered as a treatment option, and indicate that the direct use of rosiglitazone for treatment of nonalcoholic fatty liver may not be desirable when the patient's PPAR-γ level in the liver is significantly elevated.

KEY WORDS: NAFLD; nuclear receptor; obesity; peroxisome proliferator-activated receptors; rosiglitazone.

INTRODUCTION

Rosiglitazone is an insulin sensitizer for the treatment of type 2 diabetes. In addition to improving insulin sensitivity, rosiglitazone influences the pathological conditions of nonalcoholic fatty liver disease (NAFLD). It has been shown that rosiglitazone decreases the hepatic triglyceride content in Otsuka Long-Evans Tokushima Fatty rats (1). Beneficial effects have also been reported on many other animal models (2,3). In humans, recent clinical studies reveal that rosiglitazone improves NAFLD (4,5), thus supporting the use of rosiglitazone in treating this disease. However, it has also been reported that rosiglitazone can actually exacerbate NAFLD (6–8). For instance, treatment of KKAy diabetic mice with rosiglitazone resulted in severe liver steatosis (6). Similar deleterious effects have also been reported on *ob*/*ob* mice with or without deficiency of the low-density lipoprotein receptor gene (7,8).

Nuclear receptor peroxisome proliferator-activated receptor gamma (PPAR-γ) plays an important role in the rosiglitazone-induced increase of insulin sensitivity (9–11). Its activity also affects adipogenesis and hepatic fat homeostasis (9). It has been previously shown that overexpression of PPAR-γ *via* an adenoviral vector leads to ectopic fat deposition in the liver, while liver-specific disruption of the PPAR-γ pathway improves hepatic steatosis (12,13). Results from previous studies have linked aberrant PPAR-γ expression and/or PPAR-γ polymorphism to NAFLD development, underscoring the importance of PPAR-γ in the pathogenesis of human hepatic steatosis (14–16). These previous observations prompt us to hypothesize that the apparent contradictory effects of rosiglitazone on improving or exacerbating nonalcoholic fatty liver disease are related to the hepatic level of PPAR-γ expression. Our hypothesis posits that rosiglitazone brings benefits to NAFLD patients with a low level of PPAR-γ in the liver and exacerbates the disease when patients have an elevated level of PPAR-γ.

To test this hypothesis, we employed the technique of gene transfer to upregulate PPAR-γ gene expression in mice fed a high-fat diet (HFD) and studied the consequences of rosiglitazone treatment. We demonstrate that rosiglitazone aggravates liver steatosis when expression of *Ppar-γ* is upregulated in the liver. Conversely, rosiglitazone treatment prevents mice from developing HFD-induced fatty liver.

Electronic supplementary material The online version of this article (doi:10.1208/s12248-016-9919-9) contains supplementary material, which is available to authorized users.

[1] Department of Pharmaceutical and Biomedical Sciences, College of Pharmacy, University of Georgia, Athens, Georgia 30602, USA.
[2] To whom correspondence should be addressed. (e-mail: dliu@uga.edu)

METHODS

Animals and Materials

Male C57BL/6 mice (~22 g) were purchased from Charles River (Wilmington, MA). The high-fat diet (60% kJ/fat, #F3282) was purchased from Bio-Serv (Frenchtown, NJ). Rosiglitazone was purchased from Cayman Chemical (Ann Arbor, MI). The mouse genes of *Ppar-γ*, *Cd36*, *Fabp4*, and *Mgat1* were cloned from complementary DNA sequences of C57BL/6 mice and inserted into pLIVE plasmid vectors (Mirus Bio, Madison, WI). Primers for PCR analyses were made at Sigma-Aldrich (St. Louis, MO).

Animal Treatments

Animal treatments were performed following the approved protocol (A2014 07-008-Y1-A0) by the IACUC of the University of Georgia. The mice were housed under a standard condition with a 12-h light-dark cycle and a regular chow or high-fat diet. Intraperitoneal injection of rosiglitazone was performed on non-obese mice (~22 g) at a dose of 20 mg/kg twice weekly for 9 weeks, and a carrier solution was used as the control. A 3-week preventive study was performed by using a low dose of 5 mg/kg daily. Obese mice were obtained by HFD feeding for 16 weeks until their body weight reached ~50 g. These obese mice were treated with a lower dose of 5 mg/kg rather than 20 mg/kg, because the latter showed a significant toxicity leading to marked weight loss in obese mice (data not shown). The rosiglitazone treatment of the obese mice was performed (i.p.) daily for a total of 15 days. Gene transfer to animals was accomplished by employing the hydrodynamic tail vein injection of 10 μg plasmid DNA per mouse according to the procedure previously established (17). Control mice in this study were transferred with the backbone vector using the same procedure.

Hematoxylin and Eosin Staining and Immunofluorescence

Liver samples were freshly collected and fixed using neutrally buffered formalin for 24 h. The fixed tissue samples were then embedded into paraffin and cut 6 μm in thickness. Staining was performed using a commercial kit from BBC Biochemical (Atlanta, GA) following the protocol provided by the manufacturer. Tissue sections were examined and photographed using the NIS-Elements imaging platform from the Nikon Instruments Inc. (Melville, NY). A PPAR-γ

Table I. PCR Primer Sequences

Gene name	Forward primer sequence (F)	Reverse primer sequence (R)
Acadm	F: GGGTTTAGTTTTGAGTTGACGG	R: CCCCGCTTTTGTCATATTCCG
Acadl	F: TCTTTTCCTCGGAGCATGACA	R: GACCTCTCTACTCACTTCTCCAG
Acc	F: ATGGGCGGAATGGTCTCTTTC	R: TGGGGACCTTGTCTTCATCAT
Atgl	F: GGATGGCGGCATTTCAGACA	R: CAAAGGGTTGGGTTGGTTCAG
Cd36	F: ATGGGCTGTGATCGGAACTG	R: GTCTTCCCAATAAGCATGTCTCC
ChREBP	F: AGATGGAGAACCGACGTATCA	R: ACTGAGCGTGCTGACAAGTC
Cpt1a	F: CTCCGCCTGAGCCATGAAG	R: CACCAGTGATGATGCCATTCT
Cpt1b	F: GCACACCAGGCAGTAGCTTT	R: CAGGAGTTGATTCCAGACAGGT
Dgat1	F: TCCGTCCAGGGTGGTAGTG	R: TGAACAAAGAATCTTGCAGACG
Dgat2	F: GCGCTACTTCCGAGACTACTT	R: GGGCCTTATGCCAGGAAACT
Ehhadh	F: ATGGCTGAGTATCTGAGGCTG	R: ACCGTATGGTCCAAACTAGCTT
Fabp4	F: AAGGTGAAGAGCATCATAACCC	R: TCACGCCTTTCATAACACATTCC
Fas	F: GGAGGTGGTG ATAGCCGGTAT	R: TGGGTAATCCATAGAGCCCAG
Fxr	F: GCTTGATGTGCTACAAAAGCTG	R: CGTGGTGATGGTTGAATGTCC
Gapdh	F: AGGTCGGTGTGAACGGATTTG	R: TGTAGACCATGTAGTTGAGGTCA
Hnf4	F: CACGCGGAGGTCAAGCTAC	R: CCCAGAGATGGGAGAGGTGAT
Hsl	F: CCAGCCTGAGGGCTTACTG	R: CTCCATTGACTGTGACATCTCG
Lpl	F: GGGAGTTTGGCTCCAGAGTTT	R: TGTGTCTTCAGGGGTCCTTAG
Lxrα	F: CTCAATGCCTGATGTTTCTCCT	R: TCCAACCCTATCCCTAAAGCAA
Mgat1	F: TGGTGCCAGTTTGGTTCCAG	R: TGCTCTGAGGTCGGGTTCA
Mgat2	F: TGGGAGCGCAGGTTACAGA	R: CAGGTGGCATACAGGACAGA
Pgc1α	F: TATGGAGTGACATAGAGTGTGC	R: CCACTTCA ATCCACCCAGAAAG
Pgc1β	F: TCCTGTAAAAGCCCGGAGTAT	R: GCTCTGGTAGGGGCAGTGA
Plin1	F: GGGACCTGTGAGTGCTTCC	R: GTATTGAAGAGCCGGGATCTTTT
Ppar-α	F: AGAGCCCCATCTGTCCTCTC	R: ACTGGTAGTCTGCAAAACCAAA
Ppar-γ1	F: GGAAGACCACTCGCATTCCTT	R: GTAATCAGCAACCATTGGGTCA
Ppar-γ2	F: TCGCTGATGCACTGCCTATG	R: GAGAGGTCCACAGAGCTGATT
Ppar-δ	F: TCCATCGTCAACAAAGACGGG	R: ACTTGGGCTCAATGATGTCAC
Pxr	F: GATGGAGGTCTTCAAATCTGCC	R: GGCCCTTCTGAAAAACCCCT
Scd-1	F: TTCTTGCGATACACTCTGGTGC	R: CGGGATTGAATGTTCTTGTCGT
Srebp1c	F: GCAGCCACCATCTAGCCTG	R: CAGCAGTGAGTCTGCCTTGAT
Ucp1	F: AGGCTTCCAGTACCATTAGGT	R: CTGAGTGAGGCAAAGCTGATTT
Ucp2	F: ATGGTTGGTTTCAAGGCCACA	R: CGGTATCCAGAGGGAAAGTGAT
Ucp3	F: CTGCACCGCCAGATGAGTTT	R: ATCATGGCTTGAAATCGGACC

immunofluorescence study was performed by following the protocol provided by the antibody supplier of Cell Signaling Technology (Danvers, MA).

Determination of Hepatic Triglyceride Level

Red Oil O staining was used to assess the level and distribution of fat droplets in the liver using frozen sections of freshly collected liver samples. Frozen liver sections (8 μm) were stained with 0.2% Oil Red O in a 60% solution of isopropanol for 20 min and then washed three times with phosphate-buffered saline. A microscopic examination was performed and photographs were taken under a regular light microscope.

Quantitative determination of liver triglycerides was performed as previously described (18). Briefly, frozen liver samples (200–400 mg per sample) were homogenized in a mixed solution of chloroform and methanol (2:1) and incubated overnight at 4°C. The tissue homogenates were centrifuged at 12,000 rpm for 20 min, and the supernatants were dried and re-dissolved in a 5% solution of Triton-X100. The triglyceride concentration was determined using a commercial kit (Thermo-Scientific, Pittsburgh, PA).

Gene Expression Analyses

Total RNA was isolated using a TRIZOL reagent from Invitrogen (Grand Island, NY). Quantitative analyses of messenger RNA (mRNA) were performed using SYBR Green as a detection reagent on the ABI StepOnePlus Real-Time PCR system. Data analyses were conducted using the ΔΔCt method. GAPDH mRNA was utilized as an internal reference. Primers were synthesized at Sigma (St. Louis, MO), and their sequences are listed in Table I. Melting curve analysis of real-time PCR products was conducted and showed a single DNA duplex.

Statistical Analysis

All results were expressed as the mean ± SD. Statistical analyses were performed using Student's *t* test and ANOVA. A *p* value below 0.05 ($p < 0.05$) was considered significantly different.

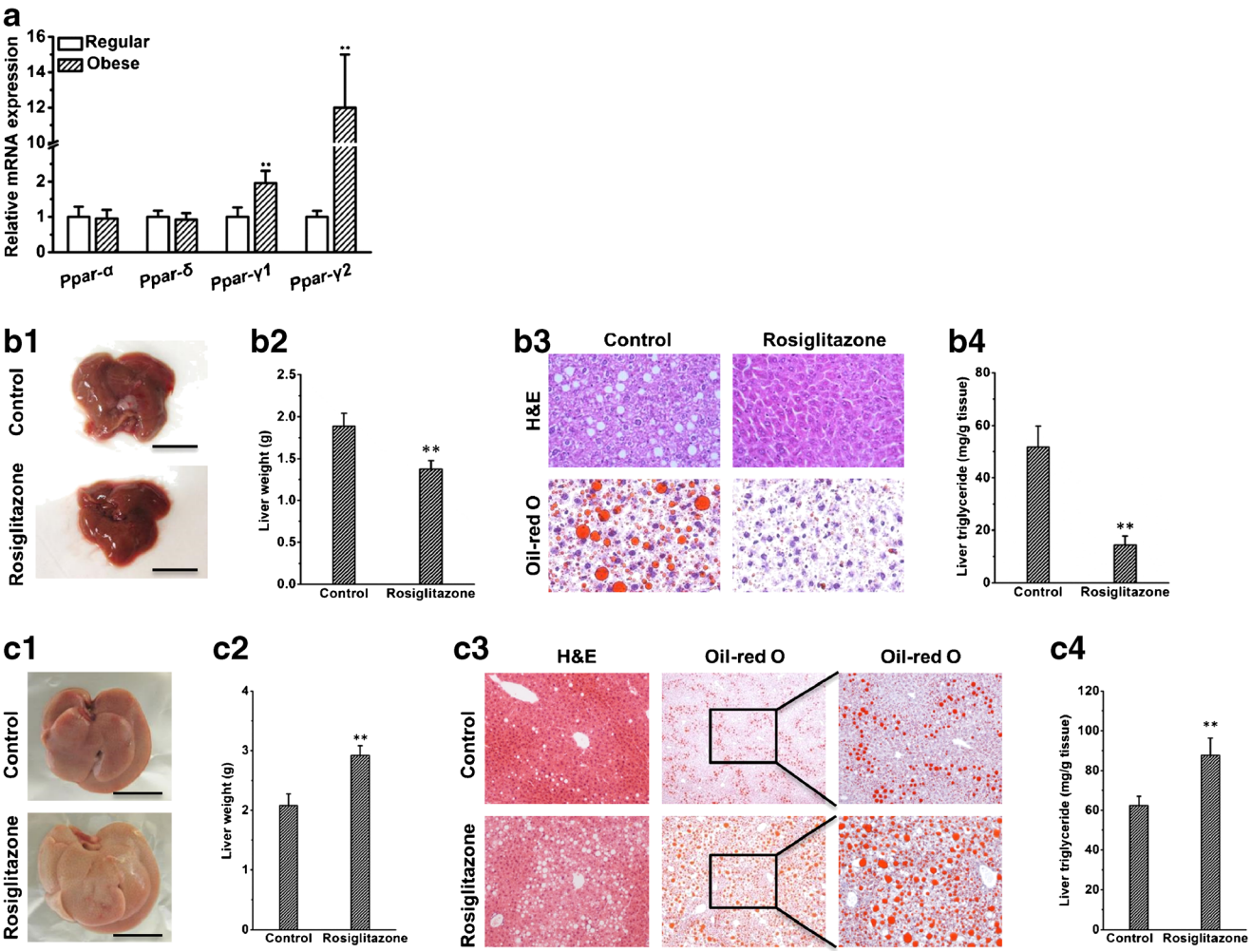

Fig. 1. Opposing effects of rosiglitazone on HFD-induced fatty liver. *A* Expression levels of PPARs in the liver of normal and obese mice; *B1* representative images of liver at the end of the prevention experiment (bar length = 1 cm); *B2* weight of liver; *B3* representative images of H&E staining and Oil red O staining of liver sections; *B4* liver triglyceride level; *C1* representative images of liver at the end of the 15-day rosiglitazone treatment of obese mice (bar length = 1 cm); *C2* weight of liver; *C3* representative images of H&E staining and Oil red O staining of liver sections; and *C4* liver triglyceride level. Values in *A*, *B2*, *B4*, *C2*, and *C4* represent average ± SD ($n = 5$). *One asterisk* $p < 0.05$ and *two asterisks* $p < 0.01$ compared with control mice

RESULTS

Impact of Rosiglitazone Treatment on Mice with Different Levels of Hepatic PPAR-γ

HFD-induced hepatic fat accumulation was employed to examine the PPAR-γ-dependent effects of rosiglitazone treatment on fat accumulation in the liver. Results in Fig. 1a show relative mRNA levels of peroxisome proliferator-activated receptors (*Ppar-α*, *Ppar-γ1*, *Ppar-γ2*, and *Ppar-δ*). The hepatic PPAR-γ1 level in obese mice is ~2-fold higher than that of normal mice. The effects of rosiglitazone treatment on the normal and obese mice were examined by means of intraperitoneal injection of rosiglitazone into mice fed a HFD. For normal mice with low or normal levels of PPAR-γ in the liver, 9 weeks of rosiglitazone treatment resulted in an average liver weight of ~1.4 g, ~27.1% lower than that of the controls injected with a carrier solution (Fig. 1(B1 and B2)). Structural analysis with hematoxylin and eosin (H&E) and Oil Red O staining revealed the presence of a significant amount of fat content in the liver of the control animals but not in the liver of rosiglitazone-treated mice (Fig. 1(B3)). A significantly lower level of hepatic lipids in rosiglitazone-treated animals was confirmed by biochemical determination (Fig. 1(B4)). A 3-week preventive study with a daily injection of a lower dose of rosiglitazone further confirmed the beneficial effect of this drug on fatty liver (Supplementary Figure 1). These results suggest that rosiglitazone treatment alleviates HFD-induced lipid accumulation in the liver.

In obese mice, those treated with rosiglitazone had a liver weight of ~2.9 g compared to ~2.1 g of the control animals injected with a carrier solution. An increase in the vacuole structure of H&E staining of the liver (Fig. 1(C1 and C2)) and the density of Oil Red O-stained lipid droplets was seen in rosiglitazone-treated obese mice (Fig. 1(C3)). Results in Fig. 1(C4) show that rosiglitazone treatment resulted in a ~140.4% increase of triglycerides in the liver. These results demonstrate the opposing effects of rosiglitazone treatment. In normal mice with a lower level of PPAR-γ expression, rosiglitazone blocked HFD-induced fatty liver. Conversely, rosiglitazone treatment exacerbated hepatic steatosis in obese mice with a higher level of PPAR-γ in the liver.

Hepatic PPAR-γ Regulates the Effect of Rosiglitazone on the Exacerbation of Ectopic Fat Deposition in the Liver

While results in Fig. 1 provide evidence in support of a correlation between the PPAR-γ level in the liver and the effect of rosiglitazone treatment on hepatic fat accumulation, we extended our effort to seek direct evidence in support of our conclusion that fat accumulation is regulated by the PPAR-γ level in the liver. To this end, we cloned the *Ppar-γ1* gene into a

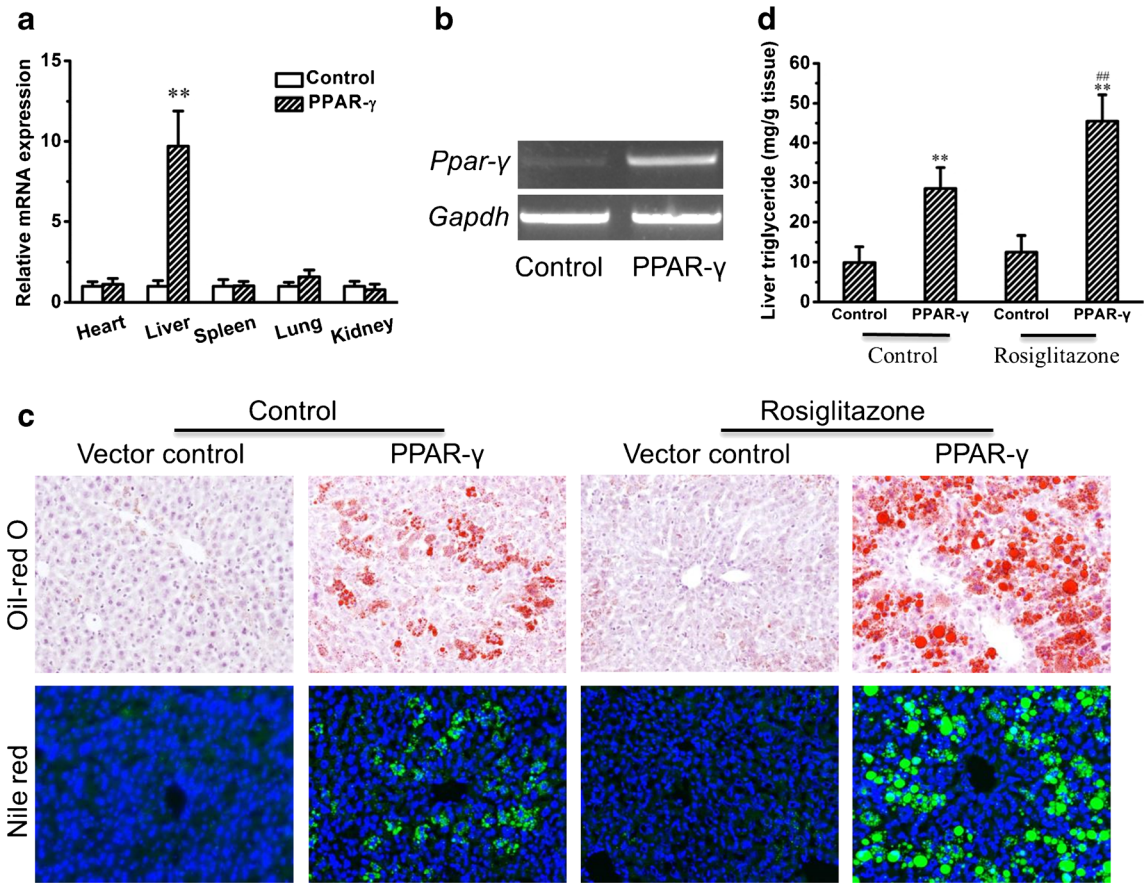

Fig. 2. Hepatic PPAR-γ controls the effect of rosiglitazone on hepatic fat deposition. **a** Expression of *Ppar-γ* in major organs 3 days after gene transfer; **b** verification of the overexpression of *Ppar-γ* in the liver; **c** representative images of Oil red O staining and Nile red staining of liver sections; and **d** liver triglyceride level. Values in **a** and **d** represent average ± SD ($n = 5$). Mice were euthanized 3 days after *Ppar-γ* gene transfer. *Asterisks* $p < 0.01$ compared to control mice without rosiglitazone treatment, *number signs* $p < 0.01$ compared with *Ppar-γ*-transferred mice without rosiglitazone treatment

plasmid vector. Its expression was driven by the hepatocyte-specific albumin promoter. We then transferred this plasmid into non-obese mice using hydrodynamics-based gene delivery (17). *Ppar-γ* gene transfer increased the mRNA level of PPAR-γ exclusively in the liver (Fig. 2a), which was verified by regular PCR (Fig. 2b). Overexpression of *Ppar-γ* in hepatocytes resulted in rapid lipid accumulation in the mouse livers, even those of mice on a standard chow. PPAR-γ and lipid droplets co-localize in hepatocytes after *Ppar-γ* gene transfer (Supplementary Figure 2). Importantly, rosiglitazone induced significant numbers of lipid droplets only in the liver cells with PPAR-γ overexpression (Fig. 2c). This conclusion was further confirmed by biochemical determinations (Fig. 2d). Taken together, these results indicate that hepatic PPAR-γ plays an important role in regulating the effect of rosiglitazone in altering pathological conditions of liver steatosis.

Impact of *Ppar-γ* Overexpression on the Expression of Genes Involved in Lipid Metabolism

We next explored the underlying mechanisms for PPAR-γ-dependent rosiglitazone-induced hepatic exacerbation as shown in Fig. 2. Real-time PCR was employed to determine the relative mRNA level of the genes known for their involvement in glucose and lipid metabolism. Results in Fig. 3 show that overexpression of *Ppar-γ* did not affect mRNA levels of nuclear receptor genes known for transcription regulation (Fig. 3a). However, expression levels of the key genes for *de novo* lipogenesis were increased with *Ppar-γ* overexpression, including *Fas* (~1.7-fold) and *Scd-1* (~2.3-fold) (Fig. 3b). No significant change was seen in the mRNA levels of crucial genes for lipid oxidation (Fig. 3c). The expression of key genes responsible for energy expenditure in the liver was not affected, with the exception of *Ucp2* which was increased ~1.6-fold (Fig. 3d). Overexpression of *Ppar-γ* led to an elevated expression of *Hsl* (~5.3-fold), *Atgl* (~2.6-fold), *Cd36* (~3.2-fold), and *Fabp4* (~11.5-fold) (Fig. 3e). Intriguingly, transfer of the *Ppar-γ* plasmids increased the expression of several pivotal genes for lipid droplet development, including *Mgat1* (~6.1-fold) and *Dgat1* (~1.7-fold) (Fig. 3f). Collectively, this set of data shows that the overexpression of *Ppar-γ* elevates the expression of a set of pivotal genes involved in hepatic lipid metabolism, particularly *Cd36*, *Fabp4*, and *Mgat1*.

Concurrent and time-dependent expressions of *Ppar-γ* after hydrodynamic gene transfer and its pivotal target genes *Cd36*, *Fabp4*, and *Mgat1* were monitored. Results in Fig. 4 show the mRNA level of the selected genes as a function of time after the *Ppar-γ* gene transfer. The mRNA level of *Ppar-γ* increased by ~9.2-fold 3 days after gene transfer and maintained at a relatively high level for over 1 month (Fig. 4a). Similar patterns were observed in the three pivotal genes regulated by PPAR-γ, including *Cd36*, *Fabp4*, and *Mgat1*. These peaked at ~8.1-fold, ~40.8-fold, and ~12.1-fold, respectively (Fig. 4b–d). Increased expressions of *Ppar-γ*, *Cd36*, *Fabp4*, and *Mgat1* were accompanied by a significantly high level of lipids in the livers of animals with *Ppar-γ* gene transfer (Fig. 4e).

Concurrent Overexpression of *Cd36*, *Fabp4*, and *Mgat1* Replicates the PPAR-γ-Mediated Hepatic Fat Deposition

We next investigated whether the three pivotal genes that are targets of PPAR-γ, *Cd36*, *Fabp4*, and *Mgat1* are responsible for hepatic fat aggregation induced by *Ppar-γ*

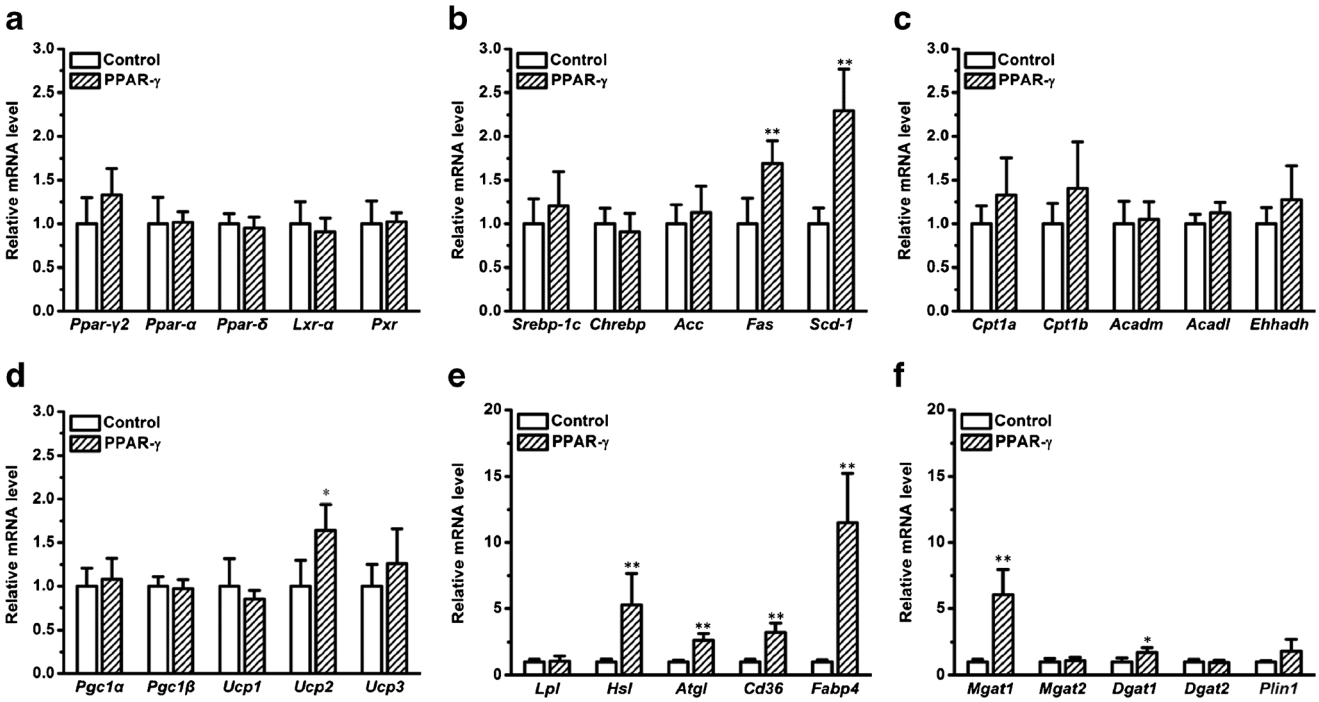

Fig. 3. Overexpression of hepatic PPAR-γ upregulated the expression of a variety of pivotal genes involved in lipid metabolism in the liver. **a** Expression of key nuclear receptor genes involved in liver lipid metabolism; **b** expression of key genes involved in de novo lipogenesis in the liver; **c** expression of key genes for fatty acid *β* oxidation; **d** expression of crucial genes for energy expenditure; **e** expression of key genes for fatty acid transport; and **f** expression of pivotal genes for lipid droplet development. Samples were collected from animals 3 days after *Ppar-γ* gene transfer. Values in **a**–**f** represent average ± SD ($n = 5$). *One asterisk* $p < 0.05$ and *two asterisks* $p < 0.01$ compared with control mice

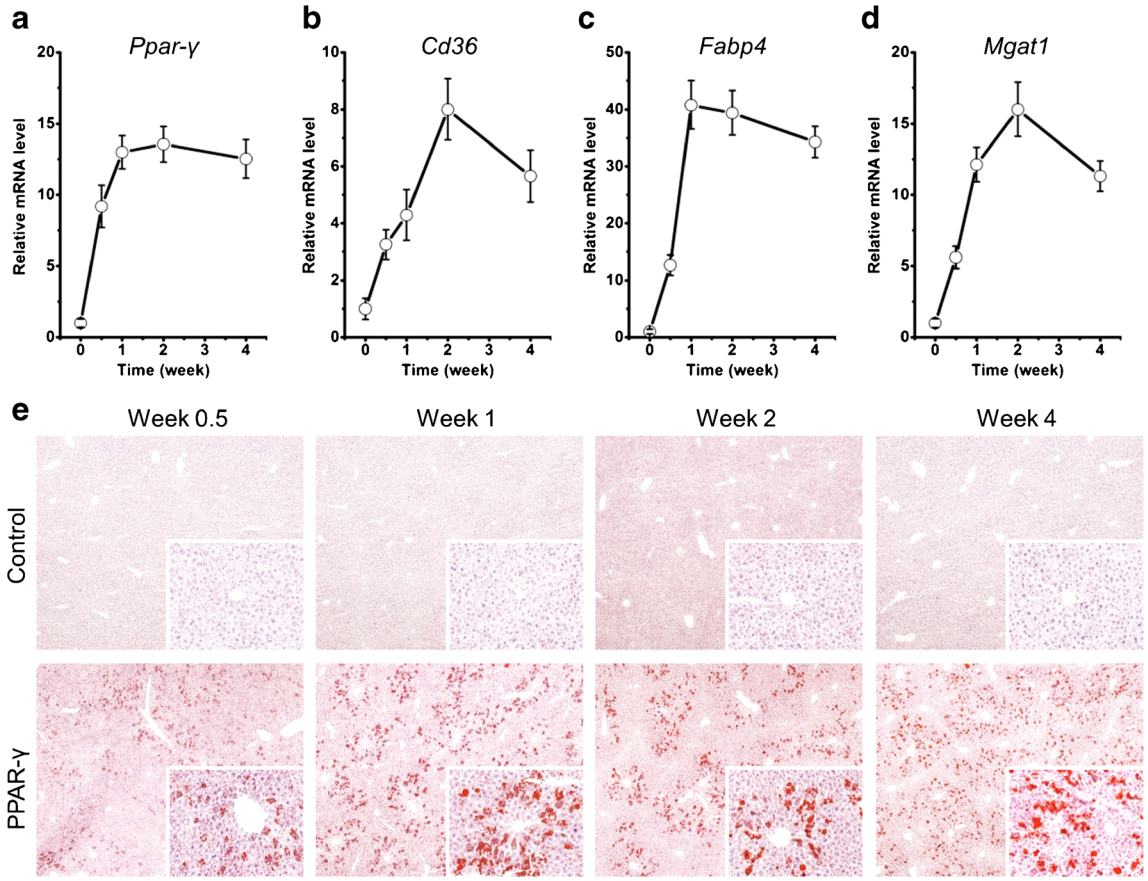

Fig. 4. The hepatic fat accumulation induced by *Ppar-γ* overexpression was associated with elevated expression of *Cd36*, *Fabp4*, and *Mgat1* in the liver. **a–d** Time-dependent mRNA levels of *Ppar-γ*, *Cd36*, *Fabp4*, and *Mgat1*, respectively, and **e** representative images of Oil red O staining of liver sections. Values in **a–d** represent average ± SD ($n = 5$)

overexpression. These three genes were cloned separately into a pLIVE plasmid vector, and the plasmids were transferred into the mouse liver together with a ratio of 1:1:1 using the same hydrodynamics-based procedure. Concurrent gene transfer greatly increased the mRNA levels of each of these three genes in the liver (Fig. 5a), which consequently led to hepatic fat aggregation in mice fed either a standard chow or a HFD (Fig. 5b). This was further verified by biochemical quantifications (Fig. 5c). Taken together, these results suggest that upregulated expression of *Cd36*, *Fabp4*, and *Mgat1* is responsible for the hepatic fat deposition induced by *Ppar-γ* overexpression.

DISCUSSION

Hepatic PPAR-γ plays an important role in maintaining lipid homeostasis in the liver. PPAR-γ was originally described as a transcriptional factor controlling adipocyte differentiation and adipogenesis (9,19). Fat-specific deletion of PPAR-γ causes lipoatrophy and severe metabolic disturbance (20). In addition to controlling adipogenesis, PPAR-γ is also involved in lipid metabolism in the liver (9,21). Convincing evidence for a critical role of PPAR-γ in hepatic lipid metabolism has been presented by taking advantage of animals with liver-specific knockout of PPAR-γ under various genetic backgrounds (13,22–24). Evidence collected from these animal models indicates that hepatic PPAR-γ is essential for ectopic fat deposition in the liver. In congruence with the phenotype of these knockout models, overexpression of PPAR-γ *via* adenoviral vectors leads to hepatic steatosis (12,25,26), although it remains unclear whether this overexpression is hepatocyte-specific. Extending these previous findings, the present study provides evidence supporting the conclusion that selective overexpression of PPAR-γ in hepatocytes is sufficient to induce rapid development of hepatic steatosis.

We demonstrate in the present study that rosiglitazone on HFD-induced NAFLD has an opposing impact for normal *vs.* obese mice (Fig. 1). While rosiglitazone treatment blocked NAFLD development in normal mice, this treatment in obese mice led to a deleterious outcome (Fig. 1C). Mechanistically, this opposing effect is related to *Ppar-γ* gene expression in the liver (Fig. 1a). Liver-specific overexpression of the *Ppar-γ* gene in mice results in hepatic fat accumulation even with regular chow (Fig. 2). At the molecular level, increased expression of hepatic PPAR-γ promoted transcription of a number of pivotal lipogenic genes particularly *Cd36*, *Fabp4*, and *Mgat1* (Figs. 3 and 4). Taken together, these findings suggest that hepatic PPAR-γ plays a critical role in regulating the effects of rosiglitazone on hepatic fat accumulation.

The preventive effect of rosiglitazone on NAFLD in HFD-fed normal mice can be attributed to systemic activation of PPAR-γ, which influences various pathways in multiple organs collectively in favor of fat deposition in the adipose tissue rather than the liver. Systemic activation of PPAR-γ affects the entire energy metabolism system since this nuclear receptor has diverse

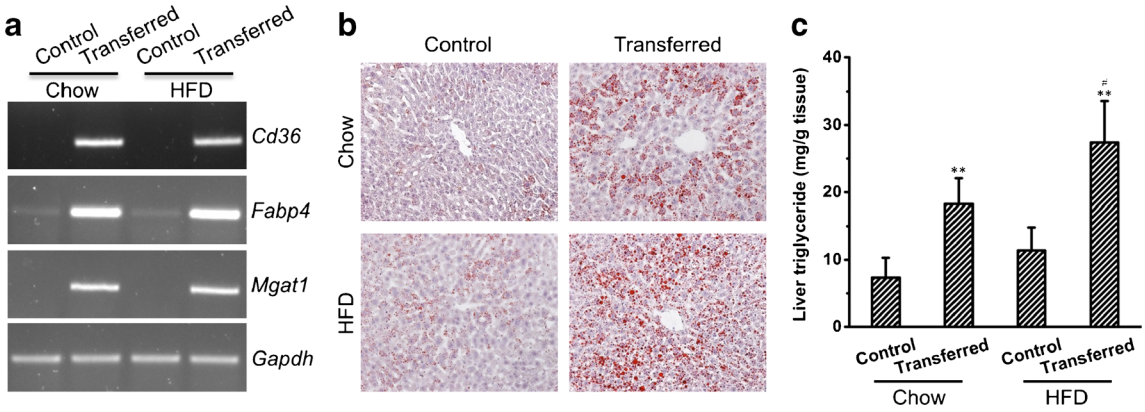

Fig. 5. Concurrent transfer of *Cd36*, *Fabp4*, and *Mgat1* genes recapitulated the phenotypic change induced by overexpression of *Ppar-γ* in the liver. **a** Verification of the concurrent overexpression of *Cd36*, *Fabp4*, and *Mgat1* in the liver; **b** representative images of Oil red O staining of the livers from mice transferred with the three pivotal genes and kept on regular chow or HFD; and **c** hepatic triglyceride level. Mice were euthanized 1 week after hydrodynamic gene transfer. Values in **c** represent average ± SD ($n = 5$). *Two asterisks* $p < 0.01$ compared with chow-fed control mice, *one number sign* $p < 0.05$ compared with *Ppar-γ*-transferred mice on chow

functions in different tissues (9). Specifically, activation of PPAR-γ in the central nervous system resulted in accelerated body weight gain (27,28); conversely, transduction of the same signal in peripheral subcutaneous fat stimulated thermogenesis and increased energy expenditure (29–33). Accordingly, the impact of the systemic administration of rosiglitazone on metabolic homeostasis is complex. In the current study, treatment with rosiglitazone blocked hepatic fat accumulation in HFD-fed mice without a significant impact on body weight gain (data not shown). In line with these findings, a recent study by Evans and colleagues showed that activation of the same pathway greatly alleviated HFD-induced hepatic steatosis in transgenic mice with adipocyte-specific overexpression of PPAR-γ (34).

The exacerbating effect of rosiglitazone in obese mice can be explained by the elevated expression of hepatic PPAR-γ, which may lead to preferential activation of PPAR-γ in the liver. It is seemingly contradictory that one drug produces distinct and opposite effects. In fact, the variable effects of rosiglitazone on NAFLD under diverse conditions have been increasingly noted, and growing evidence suggests the detrimental effect of rosiglitazone on NAFLD in diverse animal models (6–8). In agreement with these studies, our findings demonstrated that rosiglitazone markedly aggravated hepatic steatosis in HFD-induced obese mice. This was related to an elevated expression of hepatic PPAR-γ. More importantly, this liver-specific upregulation of

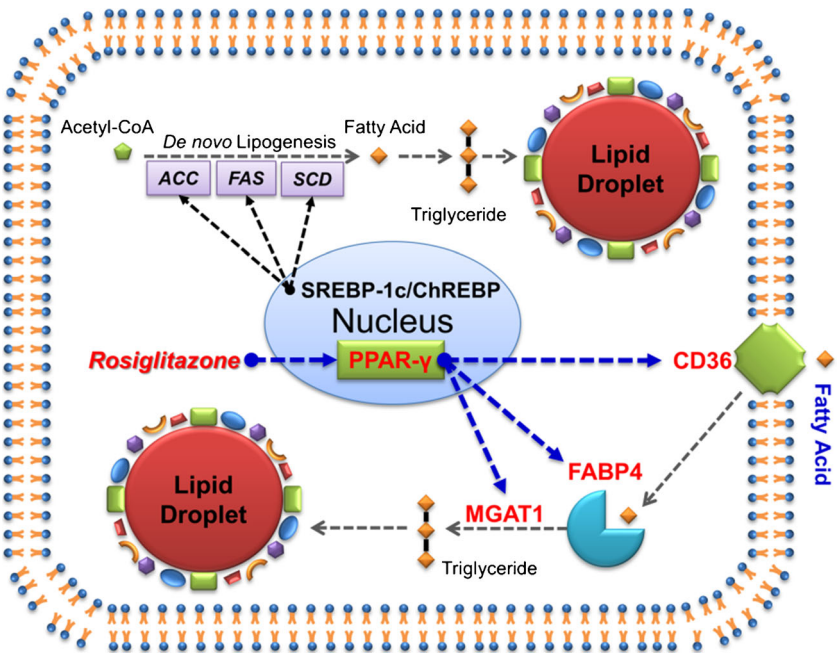

Fig. 6. Schematic diagram illustrating the possible mechanism underlying hepatic fat accumulation induced by rosiglitazone treatment and *Ppar-γ* overexpression. Rosiglitazone binds to and activates PPAR-γ. Subsequently, PPAR-γ upregulates *Cd36*, *Fabp4*, and *Mgat1*, facilitating fatty acid incorporation into triglycerides and consequently giving rise to hepatic fat aggregation as lipid droplets

PPAR-γ was indispensable in the rosiglitazone-mediated hepatic fat deposition (Figs. 1(C), 2, and 3). These findings point to the important role of elevated hepatic PPAR-γ in mediating the aggravation of hepatic steatosis by rosiglitazone. In support of this explanation, a previous study by Gonzalez and colleagues elegantly demonstrated that liver-specific deletion of PPAR-γ in *ob*/*ob* mice completely blocked rosiglitazone-induced exacerbation of hepatic steatosis (13).

The possible mechanisms underlying rosiglitazone-induced hepatic fat aggregation are depicted in Fig. 6. After administration, rosiglitazone binds to PPAR-γ and upregulates its downstream targets. Similar to those of many other nuclear receptors, the downstream signaling pathways of PPAR-γ in regulating hepatic lipid metabolism are complex and may involve multiple interrelated factors (9,35–37). In the present study, we focused on three key downstream factors and demonstrated that concurrent transfer of these three pivotal genes into mouse liver was sufficient to replicate the phenotypic alterations induced by PPAR-γ overexpression (Fig. 5), indicating that these factors contributed substantially to the dominant role of hepatic PPAR-γ in determining the effect of rosiglitazone on NAFLD. It can be speculated that increased CD36 on cell membranes facilitates intracellular transport of fatty acids, thereafter binding to FABP4, which serves as a fatty acid chaperone in cytoplasm. Subsequently, polar fatty acids are incorporated into neutral triglycerides through a group of enzymes, MGAT1 being the rate-limiting enzyme. Evidently, many other factors may also be involved in these intricate pathways (38–40), and further investigations are warranted to reveal the precise mechanisms by which overexpression of PPAR-γ rapidly increases fat accumulation in the liver.

In conclusion, the results presented in the current study show that rosiglitazone generates distinct effects on the prevention and treatment of HFD-induced NAFLD, in which hepatic PPAR-γ plays a vital role by coordinating and regulating downstream *Cd36*, *Fabp4*, and *Mgat1* in the liver. These findings suggest that caution should be taken when considering a direct application of rosiglitazone to obese patients having elevated PPAR-γ expression in the liver, and indicate that a more desirable strategy may be to activate PPAR-γ in a tissue- or cell-specific manner in order to avoid rosiglitazone-mediated exacerbation of hepatic steatosis.

ACKNOWLEDGMENTS

The study was supported in part by grants from NIH (RO1EB007357 and RO1HL098295). We thank Dr. Megan Morgan for proofreading this manuscript.

COMPLIANCE WITH ETHICAL STANDARDS

Animal treatments were performed following the approved protocol (A2014 07-008-Y1-A0) by the IACUC of the University of Georgia.

Conflict of Interest The authors declare that they have no conflicts of interest.

REFERENCES

1. Yang SJ, Choi JM, Chae SW, Kim WJ, Park SE, Rhee EJ, *et al.* Activation of peroxisome proliferator-activated receptor gamma by rosiglitazone increases sirt6 expression and ameliorates hepatic steatosis in rats. PLoS One. 2011;6(2), e17057.
2. Gupte AA, Liu JZ, Ren Y, Minze LJ, Wiles JR, Collins AR, *et al.* Rosiglitazone attenuates age- and diet-associated nonalcoholic steatohepatitis in male low-density lipoprotein receptor knockout mice. Hepatology. 2010;52(6):2001–11.
3. Zhou M, Xu A, Lam KS, Tam PK, Che CM, Chan L, *et al.* Rosiglitazone promotes fatty acyl CoA accumulation and excessive glycogen storage in livers of mice without adiponectin. J Hepatol. 2010;53(6):1108–16.
4. Ratziu V, Charlotte F, Bernhardt C, Giral P, Halbron M, Lenaour G, *et al.* Long-term efficacy of rosiglitazone in nonalcoholic steatohepatitis: results of the fatty liver improvement by rosiglitazone therapy (FLIRT 2) extension trial. Hepatology. 2010;51(2):445–53.
5. Torres DM, Jones FJ, Shaw JC, Williams CD, Ward JA, Harrison SA. Rosiglitazone *versus* rosiglitazone and metformin *versus* rosiglitazone and losartan in the treatment of nonalcoholic steatohepatitis in humans: a 12-month randomized, prospective, open- label trial. Hepatology. 2011;54(5):1631–9.
6. Bedoucha M, Atzpodien E, Boelsterli UA. Diabetic KKAy mice exhibit increased hepatic PPARgamma1 gene expression and develop hepatic steatosis upon chronic treatment with antidiabetic thiazolidinediones. J Hepatol. 2001;35(1):17–23.
7. Garcia-Ruiz I, Rodriguez-Juan C, Diaz-Sanjuan T, Martinez MA, Munoz-Yague T, Solis-Herruzo JA. Effects of rosiglitazone on the liver histology and mitochondrial function in ob/ob mice. Hepatology. 2007;46(2):414–23.
8. Rull A, Geeraert B, Aragones G, Beltran-Debon R, Rodriguez-Gallego E, Garcia-Heredia A, *et al.* Rosiglitazone and fenofibrate exacerbate liver steatosis in a mouse model of obesity and hyperlipidemia. A transcriptomic and metabolomic study. J Proteome Res. 2014;13(3):1731–43.
9. Ahmadian M, Suh JM, Hah N, Liddle C, Atkins AR, Downes M, *et al.* PPARgamma signaling and metabolism: the good, the bad and the future. Nat Med. 2013;19(5):557–66.
10. Soccio RE, Chen ER, Lazar MA. Thiazolidinediones and the promise of insulin sensitization in type 2 diabetes. Cell Metab. 2014;20(4):573–91.
11. Tontonoz P, Hu E, Spiegelman BM. Stimulation of adipogenesis in fibroblasts by PPAR gamma 2, a lipid-activated transcription factor. Cell. 1994;79(7):1147–56.
12. Yu S, Matsusue K, Kashireddy P, Cao WQ, Yeldandi V, Yeldandi AV, *et al.* Adipocyte-specific gene expression and adipogenic steatosis in the mouse liver due to peroxisome proliferator-activated receptor gamma1 (PPARgamma1) overexpression. J Biol Chem. 2003;278(1):498–505.
13. Matsusue K, Haluzik M, Lambert G, Yim SH, Gavrilova O, Ward JM, *et al.* Liver-specific disruption of PPARgamma in leptin-deficient mice improves fatty liver but aggravates diabetic phenotypes. J Clin Invest. 2003;111(5):737–47.
14. Pettinelli P, Videla LA. Up-regulation of PPAR-gamma mRNA expression in the liver of obese patients: an additional reinforcing lipogenic mechanism to SREBP-1c induction. J Clin Endocrinol Metab. 2011;96(5):1424–30.
15. Domenici FA, Brochado MJ, Martinelli Ade L, Zucoloto S, da Cunha SF, Vannucchi H. Peroxisome proliferator-activated receptors alpha and gamma2 polymorphisms in nonalcoholic fatty liver disease: a study in Brazilian patients. Gene. 2013;529(2):326–31.
16. Yang Z, Wen J, Li Q, Tao X, Ye Z, He M, *et al.* PPARG gene Pro12Ala variant contributes to the development of non-alcoholic fatty liver in middle-aged and older Chinese population. Mol Cell Endocrinol. 2012;348(1):255–9.
17. Liu F, Song Y, Liu D. Hydrodynamics-based transfection in animals by systemic administration of plasmid DNA. Gene Ther. 1999;6(7):1258–66.
18. Gao M, Bu L, Ma Y, Liu D. Concurrent activation of liver X receptor and peroxisome proliferator-activated receptor alpha exacerbates hepatic steatosis in high fat diet-induced obese mice. PLoS One. 2013;8(6), e65641.

19. Tontonoz P, Spiegelman BM. Fat and beyond: the diverse biology of PPARgamma. Annu Rev Biochem. 2008;77:289–312.
20. Wang F, Mullican SE, DiSpirito JR, Peed LC, Lazar MA. Lipoatrophy and severe metabolic disturbance in mice with fat-specific deletion of PPARgamma. Proc Natl Acad Sci U S A. 2013;110(46):18656–61.
21. Gao M, Ma Y, Cui R, Liu D. Hydrodynamic delivery of FGF21 gene alleviates obesity and fatty liver in mice fed a high-fat diet. J Control Release. 2014;185:1–11.
22. Gavrilova O, Haluzik M, Matsusue K, Cutson JJ, Johnson L, Dietz KR, *et al.* Liver peroxisome proliferator-activated receptor gamma contributes to hepatic steatosis, triglyceride clearance, and regulation of body fat mass. J Biol Chem. 2003;278(36):34268–76.
23. Zhang YL, Hernandez-Ono A, Siri P, Weisberg S, Conlon D, Graham MJ, *et al.* Aberrant hepatic expression of PPARgamma2 stimulates hepatic lipogenesis in a mouse model of obesity, insulin resistance, dyslipidemia, and hepatic steatosis. J Biol Chem. 2006;281(49):37603–15.
24. Moran-Salvador E, Lopez-Parra M, Garcia-Alonso V, Titos E, Martinez-Clemente M, Gonzalez-Periz A, *et al.* Role for PPARgamma in obesity-induced hepatic steatosis as determined by hepatocyte- and macrophage-specific conditional knockouts. Faseb J. 2011;25(8):2538–50.
25. Lee YJ, Ko EH, Kim JE, Kim E, Lee H, Choi H, *et al.* Nuclear receptor PPARgamma-regulated monoacylglycerol O-acyltransferase 1 (MGAT1) expression is responsible for the lipid accumulation in diet-induced hepatic steatosis. Proc Natl Acad Sci U S A. 2012;109(34):13656–61.
26. Matsusue K, Kusakabe T, Noguchi T, Takiguchi S, Suzuki T, Yamano S, *et al.* Hepatic steatosis in leptin-deficient mice is promoted by the PPARgamma target gene Fsp27. Cell Metab. 2008;7(4):302–11.
27. Ryan KK, Li B, Grayson BE, Matter EK, Woods SC, Seeley RJ. A role for central nervous system PPAR-gamma in the regulation of energy balance. Nat Med. 2011;17(5):623–6.
28. Lu M, Sarruf DA, Talukdar S, Sharma S, Li P, Bandyopadhyay G, *et al.* Brain PPAR-gamma promotes obesity and is required for the insulin-sensitizing effect of thiazolidinediones. Nat Med. 2011;17(5):618–22.
29. Qiang L, Wang L, Kon N, Zhao W, Lee S, Zhang Y, *et al.* Brown remodeling of white adipose tissue by SirT1-dependent deacetylation of Ppargamma. Cell. 2012;150(3):620–32.
30. Ohno H, Shinoda K, Spiegelman BM, Kajimura S. PPARgamma agonists induce a white-to-brown fat conversion through stabilization of PRDM16 protein. Cell Metab. 2012;15(3):395–404.
31. Teruel T, Hernandez R, Benito M, Lorenzo M. Rosiglitazone and retinoic acid induce uncoupling protein-1 (UCP-1) in a p38 mitogen-activated protein kinase-dependent manner in fetal primary brown adipocytes. J Biol Chem. 2003;278(1):263–9.
32. Petrovic N, Walden TB, Shabalina IG, Timmons JA, Cannon B, Nedergaard J. Chronic peroxisome proliferator-activated receptor gamma (PPARgamma) activation of epididymally derived white adipocyte cultures reveals a population of thermogenically competent, UCP1-containing adipocytes molecularly distinct from classic brown adipocytes. J Biol Chem. 2010;285(10):7153–64.
33. Pardo R, Enguix N, Lasheras J, Feliu JE, Kralli A, Villena JA. Rosiglitazone-induced mitochondrial biogenesis in white adipose tissue is independent of peroxisome proliferator-activated receptor gamma coactivator-1alpha. PLoS One. 2011;6(11), e26989.
34. Sugii S, Olson P, Sears DD, Saberi M, Atkins AR, Barish GD, *et al.* PPARgamma activation in adipocytes is sufficient for systemic insulin sensitization. Proc Natl Acad Sci U S A. 2009;106(52):22504–9.
35. Gao M, Liu D. The liver X receptor agonist T0901317 protects mice from high fat diet-induced obesity and insulin resistance. AAPS J. 2013;15(1):258–66.
36. Ma Y, Huang Y, Yan L, Gao M, Liu D. Synthetic FXR agonist GW4064 prevents diet-induced hepatic steatosis and insulin resistance. Pharm Res. 2013;30(5):1447–57.
37. Zhou J, Febbraio M, Wada T, Zhai Y, Kuruba R, He J, *et al.* Hepatic fatty acid transporter Cd36 is a common target of LXR, PXR, and PPARgamma in promoting steatosis. Gastroenterology. 2008;134(2):556–67.
38. Panasyuk G, Espeillac C, Chauvin C, Pradelli LA, Horie Y, Suzuki A, *et al.* PPARgamma contributes to PKM2 and HK2 expression in fatty liver. Nat Commun. 2012;3:672.
39. Bai L, Jia Y, Viswakarma N, Huang J, Vluggens A, Wolins NE, *et al.* Transcription coactivator mediator subunit MED1 is required for the development of fatty liver in the mouse. Hepatology. 2011;53(4):1164–74.
40. Matsusue K, Aibara D, Hayafuchi R, Matsuo K, Takiguchi S, Gonzalez FJ, *et al.* Hepatic PPARgamma and LXRalpha independently regulate lipid accumulation in the livers of genetically obese mice. FEBS Lett. 2014;588(14):2277–81.